Proceedings of the 1997 IEEE
International Conference on Robotics and Automation
Albuquerque, New Mexico - April 1997

A Singularity-Consistent Parameterization Based Direct Kinematics Algorithm for a Class of Parallel Manipulators

S. Bhattacharya D. N. Nenchev M. Uchiyama

Department of Aeronautics and Space Engineering,
Tohoku University,
Aramaki-aza-Aoba, Aoba-ku, Sendai 980-77, Japan.

Abstract

A singularity-consistent direct kinematics algorithm is a necessity for the analysis and control of parallel manipulators. The present work proposes a first order singularity consistent algorithm for a class of parallel manipulators. It is shown that the algorithm is stable, convergent and can handle the multiplicity of the direct kinematics solutions for the manipulators. The performance of the method is analyzed with the help of the numerical examples incorporated at the end of this paper.

1. Introduction

Different from serial-link manipulators, the direct kinematics of a parallel manipulator poses the problem of multiplicity of solutions [3] [4] [11]. Many researchers have been addressing the direct kinematics problem [6] [8] [11] [20], focusing mainly on a closed-form solution and on establishing the upper bound on the number of direct kinematic solutions of a generalized Stewart platform type parallel manipulator (GSPPM). Systematic studies on the subject can be obtained in [6] and [20].

Note, however, that except for some manipulators with special geometry [21], the direct kinematics problem of a parallel manipulator is generally unsolvable in closed-form. This motivated another group of researchers to propose some numerical algorithms for this purpose [7] [8] [17]. In their recent work, McAree and Daniel [9] pointed out that the major shortcoming of all those numerical methods is that they are not singularity consistent. The authors proposed three singularity consistent algorithms for 3-3 and 3-6 GSPPMs. Despite various merits of these three algorithms, they are difficult to be employed for other types of parallel manipulators. The main reason of that is the extensive dependence of these algorithm on the geometries of 3-3 and 3-6 GSPPMs.

On the other hand, with regard to nonredundant serial-link manipulators, it was pointed out [16] that motion can be initialized at a singularity. An algorithm for path tracking close to or through codimension one singularities of the inverse kinematics was developed by Kieffer [5]. An algorithm for iterative inverse kinematic solution, able to terminate at a singularity, was proposed by Tchoń and Dulęba [18]. Narashiman and Kumar [12] proposed a second order analysis to analyze the motion of a serial manipulator near its singularity. Based on a null space framework, we introduced the *singularity-consistent* (SC) method [13] [14], which has been successfully applied to both serial and parallel manipulators [15] within a reference path tracking framework. We paid attention also to the case when the path passes through singularities of the direct kinematics.

In this paper we address the problem of iterative numerical solution of the direct kinematics problem for parallel manipulators. We aim at deriving a real-time algorithm that finds a proper solution, also "beyond" the singularity manifold. The algorithm is based on the SC method, such that the iterative numerical direct kinematics problem is recast as a path tracking one. Our algorithm can be used consistently near and away from singularities for a *class* of parallel manipulators.

2. Direct Kinematics Problem

2.1. Direct Kinematics and Singularity

The direct kinematics problem of a n dof nonredundant parallel manipulator involves the determination of a point $\mathbf{x}$ in the workspace $\mathcal{W} \in \Re^n$ for a given value $\boldsymbol{\theta}$ in the actuated joint space $\mathcal{T} \in \Re^n$ of the manipulator such that

$$\mathbf{f}(\mathbf{x}, \boldsymbol{\theta}) = \mathbf{0}, \tag{1}$$

0-7803-3612-7-4/97 $5.00 ©1997 IEEE

where, $\mathbf{f} \in \Re^n$ is the nonlinear kinematic map of the manipulator [2]. Since it is rarely possible to find a $\mathbf{g}(\boldsymbol{\theta})$ such that

$$\mathbf{f}(\mathbf{g}(\boldsymbol{\theta}), \boldsymbol{\theta}) = \mathbf{0},$$

a numerical solution of eq. (1) is generally searched within $\mathcal{W}$. Most of the conventional algorithms for solving the above numerical problem start from a guess solution and iterate to converge to the actual one [9]. These algorithms depend on the differentials of the kinematic map. From eq. (1), we have

$$\mathbf{J}_p d\mathbf{x} - \mathbf{J}_s d\boldsymbol{\theta} = \mathbf{0}, \tag{2}$$

where, $\mathbf{J}_p = (\partial \mathbf{f}/\partial \mathbf{x}) \in \Re^{n \times n}$ and $\mathbf{J}_s = -(\partial \mathbf{f}/\partial \boldsymbol{\theta}) \in \Re^{n \times n}$. At the singular points of the map, the rank $\mathbf{J}_p$ and/or $\mathbf{J}_s$ become(s) smaller than n [2] which can be identified by

$$\det \mathbf{J}_p = 0 \tag{3}$$

$$\text{and/or } \det \mathbf{J}_s = 0. \tag{4}$$

Equation (3) and eq. (4) generally define analytic manifolds of co-dimensions varying from one to the maximum possible nullity of $\mathbf{J}_p$ or $\mathbf{J}_s$. These singular manifolds partition $\mathcal{W}$ into a number of open compartments. In the vicinity of a singular manifold of co-dimension one, two adjacent compartments of $\mathcal{W}$ often contain two points which map at the same point in $\mathcal{T}$.

2.2. Multiplicity of the Solutions

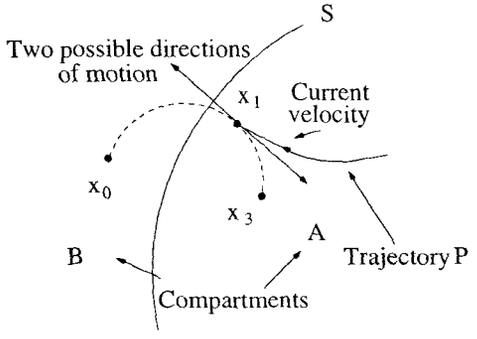

Figure 1. Multiple solutions across a singular manifold.

Figure 1 shows a singular manifold S that locally divides $\mathcal{W}$ into two open compartments A and B. Let $\mathbf{x}_0$ and $\mathbf{x}_3$ denote the two direct kinematic solutions corresponding to $\boldsymbol{\theta}_0$. Let us consider a parallel manipulator moving along a trajectory P that crosses S. After reaching $(\mathbf{x}_1, \boldsymbol{\theta}_1)$ on the trajectory, the control program of the manipulator has to solve the direct kinematics problem at the next point $\boldsymbol{\theta}_0$. But, when a conventional algorithm, starting from $\mathbf{x}_1$, searches for the solution, it cannot find both $\mathbf{x}_0$ and $\mathbf{x}_3$. The algorithm always stays within the region of attraction of $\boldsymbol{\theta}_0$ i.e., the compartment A in the present case. However, it is clear from Fig. 1 that in the above situation, the convergence to $\mathbf{x}_3$ may cause unacceptable accelerations due to the abrupt change of the direction of motion on the trajectory and subsequently the trajectory control program may fail.

Explained above is the problem related to the multiplicity of the direct kinematic solutions which is difficult to be tackled by conventional direct kinematic algorithms which are neither singularity-consistent nor formulated to find multiple solutions in line with the requirement of the trajectory controller. The problem of multiple solutions is not limited to the region near singularity. Parenti-Castelli [4] has shown that the multiple solutions may also occur within a single compartment like A.

In the subsequent part of this paper we describe a singularity-consistent direct kinematics algorithm which can not only find two solutions in the abovementioned situation but also can choose a proper solution depending on the current workspace velocity. However, the applicability of the algorithm is limited to the manipulators which do not contain a point satisfying eq. (4) in the interior of their workspace and to the other parallel manipulators which, while solving the direct kinematics problem, can be transformed into an equivalent manipulator of the previous type.

3. The Direct Kinematics Algorithm

3.1. Formulation

Let $\boldsymbol{\theta}_0$ be the point at which the direct kinematics problem for the parallel manipulator has to be solved, $\mathbf{x}_1$ be the initial guess to the algorithm, and $\boldsymbol{\theta}_1 \in \mathcal{T}$ be such that

$$\mathbf{h}(\mathbf{x}_1) = \boldsymbol{\theta}_1. \tag{5}$$

$\mathbf{h} \in \Re^n$ is the inverse kinematic function of the manipulator, which can be easily obtained in closed form. We define a linear parameterization in $\mathcal{T}$ according to

$$\boldsymbol{\theta}(s) = \boldsymbol{\theta}_1 + (\boldsymbol{\theta}_0 - \boldsymbol{\theta}_1)s \quad \text{for } 0 \leq s \leq 1. \tag{6}$$

Equation (6) defines an one-dimensional submanifold $\boldsymbol{\theta}(s) \in \mathcal{T}$. We assume that at any singularity encountered on the path, the map $\mathbf{h}(\mathbf{x})$ is transversal to $\boldsymbol{\theta}(s)$ [1]. Therefore,

$$\text{Im}(\partial \mathbf{h}(\mathbf{x})/\partial \mathbf{x}) + T_{h(x)}\boldsymbol{\theta}(s) = \Re^n. \tag{7}$$

The transversability condition in eq. (7) implies that at a singularity, $(\partial \boldsymbol{\theta}/\partial s)$ is linearly independent of the

columns of $(\partial \mathbf{h}(\mathbf{x})/\partial \mathbf{x})$ which is equal to $\mathbf{J}_s^{-1}\mathbf{J}_p$ (ref. eq 2). Another important assumption we make is that $\mathbf{J}_s$ has always full rank. Therefore we can conclude that eq. (7) implies that $\partial \mathbf{f}/\partial s$ is always independent of the columns of $\mathbf{J}_p$ at a codimension one singularity where eq. (3) holds.

The parametrization of the path need not be always linear but the transversability condition must be satisfied at any point. In addition, the parameterization should not introduce any singularity: $\boldsymbol{\theta}(s)$: $(\partial\boldsymbol{\theta}(s)/\partial s) \neq \mathbf{0}$ for $s < 1$.

Rewrite eq. (2) as:

$$\mathbf{H}d\mathbf{q} = \mathbf{0} \tag{8}$$

where, $\mathbf{H} = [\mathbf{J}_p \; -\mathbf{j}_s] \in \Re^{n\times(n+1)}$, $\mathbf{j}_s = \mathbf{J}_s\,(\boldsymbol{\theta}_0 - \boldsymbol{\theta}_1)$ and $d\mathbf{q} = [d\mathbf{x}^t \; ds]^t$. Note that because of the assumption of full rankness of $\mathbf{J}_s$, $\mathbf{j}_s$ never vanishes. It can be easily verified [14] that the solution

$$d\mathbf{q} = b\boldsymbol{\nu}(\mathbf{q}) \tag{9}$$

satisfies eq. (8), where, $\boldsymbol{\nu} \in \mathcal{N}(\mathbf{H})$ and b is an arbitrary scalar; $\mathcal{N}(\circ)$ denotes the null space of a matrix. The last equation determines a vector field over $\mathcal{T}$.

3.2. Singularity Consistency

Following the SC method [13] (cf. also [18]), we define,

$$\boldsymbol{\nu}(\mathbf{q}) = \left\{ \begin{array}{c} (\mathrm{adj}\,\mathbf{J}_p)\mathbf{j}_s \\ \det \mathbf{J}_p \end{array} \right\}. \tag{10}$$

Exactly at a singular point of codimension one, $\dot{s} = \det \mathbf{J}_p = 0$, $Im\ (\mathrm{adj}\mathbf{J}_p) = \mathcal{N}(\mathbf{J}_p)$, $\mathbf{j}_s \neq \mathbf{0}$ for $s < 1$ and $rank(\mathrm{adj}\ \mathbf{J}_p) = 1$. So $\mathrm{rank}((\mathrm{adj}\ \mathbf{J}_p)[\mathbf{J}_p \; -\mathbf{j}_s]) = 1$. Now since $(\mathrm{adj}\ \mathbf{J}_p)\mathbf{J}_p$ is a null matrix at a singularity,

$$(\mathrm{adj}\mathbf{J}_p)\mathbf{j}_s \neq \mathbf{0}$$
$$\text{and } (\mathrm{adj}\ \mathbf{J}_p)\mathbf{j}_s \in \mathcal{N}(\mathbf{J}_p)$$

which in turn implies that $\dot{\mathbf{q}} \neq \mathbf{0}$ at the singular point. Therefore, the manipulator is consistent at a singular point encountered on the path and it can also escape the singularity.

3.3. Stability

In order to check the stability of the system represented by eq. (9) on $\boldsymbol{\theta}(s)$, we construct the following Liapunov function.

$$V = \frac{1}{2}\mathbf{e}^t\mathbf{K}\mathbf{e}$$

where $\mathbf{e} = (\boldsymbol{\theta} - \boldsymbol{\theta}_0 s)$ is the perturbation on the path and $\mathbf{K} \in \Re^{n\times n}$ is a positive definite diagonal matrix. Note that we have shifted the origin to $\boldsymbol{\theta}_1$. Next, we differentiate the Liapunov function and substitute eq. (2) and eq. (9) in the resulting derivative to obtain,

$$\dot{V} = -\mathbf{e}^t\mathbf{K}\mathbf{J}_s^{-1}\mathbf{H}\dot{\mathbf{q}}. \tag{11}$$

When $\dot{\mathbf{q}}$, obtained from eq. (9), is substituted in the above expression, $\dot{V}$ becomes zero. That shows that the motion along the path is not asymptotically stable. In order to make the motion asymptotically stable we use an approach as in [14], [15] to compensate for the path perturbation. We define,

$$\dot{\mathbf{q}} = b\boldsymbol{\nu}(\mathbf{q}) + \mathbf{H}^+\mathbf{J}_s\mathbf{e}, \tag{12}$$

Substituting $\dot{\mathbf{q}}$ from eq. (12) in eq. (11) and using the fact that $\mathbf{H}\mathbf{H}^+$ is an identity matrix under eq. (7), we obtain

$$\dot{V} = -\mathbf{e}^t\mathbf{K}\mathbf{e}.$$

Therefore, $\dot{V} < 0$ and the closed loop system satisfying eq. (12) becomes asymptotically stable on $\boldsymbol{\theta}(s)$.

3.4. Convergence

For establishing the convergence of the algorithm, we assume $\mathbf{e} = \mathbf{0}$. The convergence is ensured if the open loop system mentioned above always moves towards $\boldsymbol{\theta}_0$. In order to show that, we propose a candidate Liapunov function

$$U = \frac{1}{2}(\boldsymbol{\theta}_0 - \boldsymbol{\theta}(s))^t\mathbf{Q}(\boldsymbol{\theta}_0 - \boldsymbol{\theta}(s)),$$

where, $\mathbf{Q} \in \Re^{n\times n}$ is a positive definite diagonal matrix. Taking the time derivative of U we obtain,

$$\dot{U} = -(1-s)\boldsymbol{\theta}_1^t\mathbf{Q}\boldsymbol{\theta}_1\dot{s}.$$

When the solution of $\dot{s}$ from eq. (9) is substituted in the above equation, we obtain

$$\dot{U} = -(1-s)\boldsymbol{\theta}_1^t\mathbf{Q}\boldsymbol{\theta}_1 b(\det \mathbf{J}_p).$$

Since $(1-s)\boldsymbol{\theta}_1^t\mathbf{Q}\boldsymbol{\theta}_1 > 0$ for $s < 1$, the above expression clearly shows that the algorithm is convergent if $b\det \mathbf{J}_p > 0$.

It is well known that the sign of $(\det \mathbf{J}_p)$ cannot change within a compartment like A in Fig. 1 and the sign changes across a singular manifold separating two compartments like A and B in Fig. 1. Therefore, a convergent algorithm can only move towards the solution in the same compartment. However, a divergent algorithm with $b(\det \mathbf{J}_p) < 0$ moves toward the opposite direction and crosses the singular manifold to find the other solution. In practical applications, the sign of b should be chosen to maintain the continuity of

velocity of the parallel manipulator in workspace coordinates consequently, the algorithm automatically selects the proper solution.

After the discussion about singularity consistency, stability and convergence, we state the final form of the first order algorithm which is given below:

$$\mathbf{q}_0 - \mathbf{q}_1 = \int_{t=0,s=0}^{s=1} \left(b\boldsymbol{\nu}(\mathbf{q}) + \mathbf{H}^{+}\mathbf{J}_s\mathbf{e}\right) dt. \qquad (13)$$

The quantity $\mathbf{q}_0$ contains the solution of the direct kinematic problem at $\boldsymbol{\theta}_0$. Any numerical scheme for integration may be employed to perform the integration in eq. (13) and $\mathbf{q}_0$ can be readily obtained from that.

4. Examples of the Parallel Manipulators

In this present section, we will furnish the examples of the parallel manipulators to which the present algorithm can be applied. Figure 2(a) and (b) show two

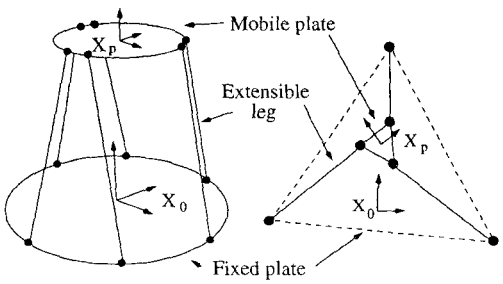

(a) Spatial, 6 dof (b) Planar, 3 dof

Figure 2. Schematic view of GSPPM.

GSPPMs, one 6 dof, spatial another 3 dof and planar. It can be easily shown that the interior of the workspace of a GSPPM is free from singularities satisfying eq. (4). There are some points on the boundary of the workspace of the manipulator at which the length of at least one of the legs of the GSPPM is zero. At those points eq. (4) is satisfied but we can neglect those singularities while considering the present algorithm. And we can conclude that any GSPPM belongs to the class to which the proposed algorithm can be applied.

Figure 3(a) shows the parallel manipulator, HEXA [19] and Fig. 3(b) shows another planar parallel manipulator [10]. The manipulator in Fig 3(a) can be conceived as a spatial version of the parallel manipulator in Fig. 3(b). They have similar kinematic characteristics. Hereafter, we will refer both the manipulators by HEXA type parallel manipulators. Given the

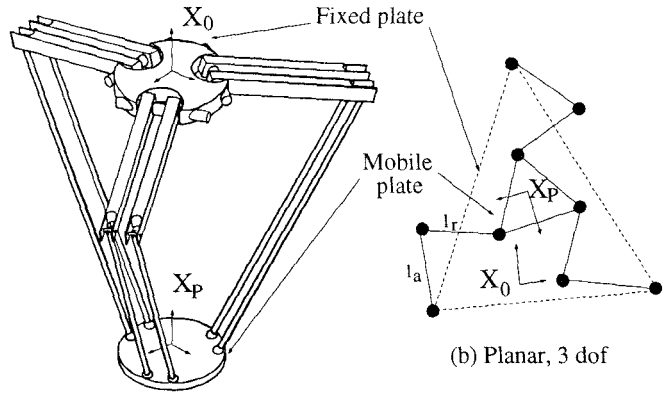

(a) HEXA, 6 dof (b) Planar, 3 dof

Figure 3. HEXA type parallel manipulators.

joint angles of a HEXA type parallel manipulator, one can replace the fixed plate and the links attached to it with the help of an equivalent rigid body. This replacement makes a HEXA an equivalent GSPPM. *The direct kinematic problem of the equivalent GSPPM can be solved to get the solution for the HEXA type manipulator.* Therefore, the HEXA type parallel manipulators can be also included in the class to which the present algorithm can be applied.

5. Numerical Examples

For the numerical example, we selected a planar HEXA type parallel manipulator with $l_r = l_a = 7$ cm (see Fig. 3 (b)). The mobile and the fixed plates of the manipulator were chosen as equilateral triangles with the sides equal to 10 cm and 20 cm, respectively. The axes system, $\mathbf{X}_p$ and $\mathbf{X}_0$ were respectively attached to the centroids of the mobile and the fixed plates. The position and orientation of $\mathbf{X}_p$ with respect to $\mathbf{X}_0$ were denoted by $[x\ y\ \phi]^t$. The position is measured in cm and the angle ϕ is in radian. We performed the integrations in eq. (13) by fourth order Runge-Kutta method and solved the examples on a SUN workstation.

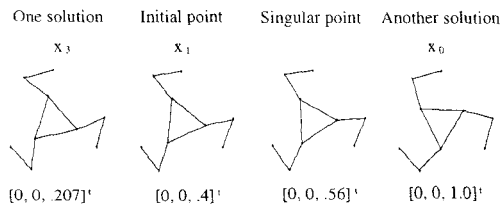

Figure 4. Different configurations of the planar parallel robot.

It can be shown [10] that a singular manifold satisfying eq. (3) passes through $x = 0$, $y = 0$ and $\phi = 0.575$ in the workspace of the manipulator in Fig. 3 (b). The joint angles at the above-mentioned singular point are $[1.166, -0.928, -3.023]^t$. We considered a case where multiplicity of the solution plays an important role. We chose $[1.292, -0.802, -2.896]^t$ as the joint angles at which the direct kinematics problem had to be solved and the corresponding initial guess was $\mathbf{x}_1 = [0.0, 0.0, 0.4]^t$. We found two direct kinematic solutions, $\mathbf{x}_3 = [0.0, 0.0, 0.207]^t$ and $\mathbf{x}_0 = [0.0, 0.0, 1.000]^t$ for the problem with the help of the proposed algorithm. Figure 4 shows the initial guess, the two solutions and the singular configuration of the manipulator. In this section our objective is to demonstrate how, under two different intial conditions at $\mathbf{x}_1$, the proposed algorithm converges to the two solutions mentioned above.

The two solutions shown in Fig. 4 were obtained by using the negative and positive values of b in eq. (13). The workspace initial velocities at $(\mathbf{x}_1, \boldsymbol{\theta}_1)$ corresponding to these negative and positive values of b were equal in magnitude but opposite in directions. In the present work, the workspace velocities were only in ϕ direction. The negative and positive $\dot{\phi}$ at the initial guess point actually correspond to the velocities away from and towards the singular manifold, respectively. In the next few paragraphs we will present the variations of $\det \mathbf{J}_p$ and $\dot{s}$ as the algorithm, started with two opposite workspace velocities, converged to two different solutions.

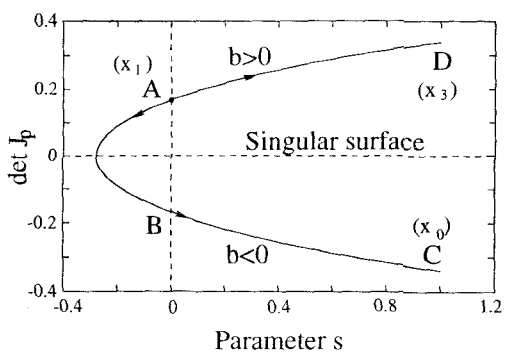

Figure 5. Determinant of $\mathbf{J}_p$ along s.

Figure 5 shows the variations of $\det \mathbf{J}_p$ with s in the above-mentioned two cases. The curves AD and ABC in the figure are the plots corresponding to the negative and positive initial values of $\dot{\phi}$, respectively, which were achieved by applying $b = 0.5$ and $b = -0.5$. The corresponding variations of $\dot{s}$ is shown by the curves NO and $LMNO$ in the phase plot, Fig. 6. It

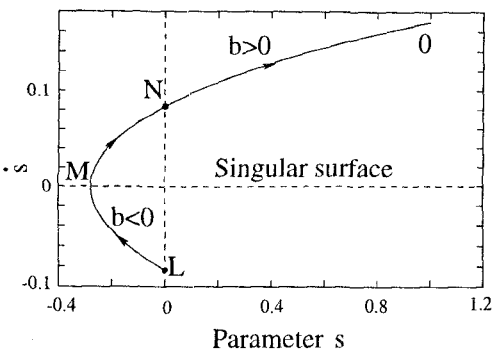

Figure 6. Phase plot for the proposed algorithm.

is clear from AD in Fig. 5 and Fig. 4 that $b = 0.5$ produced negative initial velocity along ϕ direction. Consequently, the algorithm moved from A to the final point D ($\mathbf{x}_0 = [0.0, 0.0, 0.207376]^t$) which is in the same compartment. The line segment NO in Fig. 6 shows the variation of $\dot{s}$ along the path s. It is clear from the above figures that $\dot{s}$ for $b = 0.5$ was always positive. Moreover, the algorithm always moved toward $s = 1$ and hence it was always convergent.

On the other hand, $b = -0.5$ produced positive $\dot{\phi}$ and negative $\dot{s}$. For that negative value of b, the algorithm initially moved towards the singularity as can be observed from AB in Fig. 5. The corresponding line segment LM in Fig. 6 reveals that the algorithm moved away from $s = 1$ and hence it was divergent at this stage. As the algorithm approached the singular manifold, $\dot{s}$ reduced and ultimately became zero on the singular manifold at $x = 0$, $y = 0$ and $\phi = 0.575360$. Then, the algorithm crossed the singular manifold and entered the adjacent compartment. Figure 5 shows that $\det \mathbf{J}_p$ is negative in the adjacent compartment. Once the singular manifold is crossed, the algorithm with $b = -0.5$ started converging to $s = 1$. That convergence was possible because the change of sign of $\det \mathbf{J}_p$ across the singular manifolod made the product $b \det \mathbf{J}_p$ positive. From N to O, in Fig. 6, the phase plots of the algorithm with $b = -0.5$ and $b = 0.5$ are identical.

Figure 1 shows a continuous path $\mathbf{x}_0\mathbf{x}_1\mathbf{x}_3$ (shown by the dotted line) between two direct kinematic solutions of $\boldsymbol{\theta}_0$. Many other continuous paths connecting $\mathbf{x}_0$ $\mathbf{x}_1$ and $\mathbf{x}_3$ can be constructed between $\mathbf{x}_0$ and $\mathbf{x}_3$. Two ends of all such paths are mapped onto $\boldsymbol{\theta}_0$ in $\boldsymbol{\theta}$ space. At the point $\boldsymbol{\theta}_1$ on that mapping of $\mathbf{x}_0\mathbf{x}_1\mathbf{x}_3$ in the $\boldsymbol{\theta}$ space, there exist two possible ways of reaching $\boldsymbol{\theta}_0$. The solution of the direct kinematics is determined by the way in which the final point $\boldsymbol{\theta}_0$ is reached. The sign of b is useful in choosing one of these two ways

and hence it is useful in choosing the solution of the direct kinematics. If the sign of b is such that

$$\operatorname{sgn}(\det \mathbf{J}_p)\operatorname{sgn}(b) > 0$$

at $\boldsymbol{\theta}_1$, then the algorithm is always convergent and remains in the same compartment while the opposite sign of b forces the algorithm to move in the opposite direction to find the other solution. Once the current velocity on the path is specified, b can be uniquely chosen and the corresponding direct kinematic solution can be uniquely found out.

6. Conclusion

In the present work, we developed a singularity consistent direct kinematics algorithm for a class of parallel manipulators. Our major aim was to formulate an algorithm that can resolve the problems related to the multiplicity of the direct kinematic solutions of the manipulator. Towards this goal, we analyzed the potential problem due to the multiplicity and developed one first order algorithm for solving it. Even though the algorithm is not completely general, it has been shown that if the transversality condition of the path is satisfied on the singular manifold, the proposed algorithm is stable, convergent and consistent at a singular point. It has been also shown that the algorithm can efficiently handle the problem related to the multiplicity of direct kinematic solutions in parallel manipulators easily by selecting the sign of a scalar parameter. Our future work will be directed towards removing the restriction of transversality.

References

[1] Golubitsky, M., Guillemin, V., *Stable Mappings and Their Singularities*, Springer-Verlag, 1973.

[2] Gosselin, C., Angeles, J., "Singularity Analysis of Closed-Loop Kinematic Chains," *IEEE Trans. Robotics and Automat.*, Vol. 6, No. 3, pp. 281–289, 1990.

[3] Hunt, K.H., Primrose, E.F.J., "Assembly Configurations of Some In-Parallel-Actuated Manipulators," *Mech. Mach. Theory*, Vol. 28, No. 1, pp. 31–42, 1993.

[4] Innocenti, C., Parenti-Castelli, V., "Singularity-Free Evaluation from One Configuration to Another in Serial and Fully Parallel Manipulators," *Proc. ASME Mechanisms Conf.*, Vol. DE-45, pp. 553–560, 1993.

[5] Kieffer, J., "Manipulator Inverse Kinematics for Untimed End-Effector Trajectories with Ordinary Singularities," *Int. J. Robotics Res.*, Vol. 11, No. 3, pp. 225–237, 1992.

[6] Lazard, D., *Computational Kinematics* (J. Angeles, J. Homel and P. Kovacs eds.), Kluwer, Dordrecht, pp. 175–181, 1993.

[7] Liu, K., Fitzerald, J.M., Lewis, F.L., "Kinematics Analysis of a Stewart Platform Manipulator," *IEEE Trans. Ind. Electron.*, Vol. 40., 1993.

[8] Merlet, J.-P., "Direct Kinematics and Assembly Modes of Parallel Manipulators," *Int. J. Robotics Res.*, Vol. 8, No. 5, pp. 150–162, 1992.

[9] McAree, P.R., Daniel, R.W., "A Fast, Robust Solution to the Stewart Platform Forward Kinematics," *Int. J. Robotics Res.*, Vol. 13, No. 7, pp. 407–427, 1996.

[10] Mohammadi, D.H.R., Zsomber-Murray, P.J., Angeles, J., "Singularity Analysis of Planar Parallel Manipulators," *Mech. Mach. Theory*, Vol. 30, No. 5, pp. 665–678, 1995.

[11] Nanua, P., Waldron K.J., "Direct Kinematic Solution of a Stewart Platform," *Proc. IEEE Int. Conf. on Robotics and Auto.*, pp. 431–437, 1989.

[12] Narasimhan, S., Kumar, V., "A Second Order Analysis of Manipulator Kinematics in Singular Configuration," *23rd Biennial Mech. Conf.*, pp. 477–484, 1994.

[13] Nenchev, D.N., "Tracking Manipulator Trajectories with Ordinary Singularities: a Null Space Based Approach," *Int. J. Robotics Res.*, pp. 399–404, 1995.

[14] Nenchev, D.N., Uchiyama, M., "Singularity Consistent Path Tracking: a Null Space Based Approach," *Proc. IEEE Int. Conf. on Robotics and Auto.*, pp. 2482-2489, 1995.

[15] Nenchev, D.N., Uchiyama, M., "Singularity-Consistent Path Planning and Motion Control Through Instanteneous-Self-Motion Singularities of Parallel-Link Manipulators," *J. Robotic Syst.*, Vol. 14, pp. 27–36, 1997.

[16] Nielsen, L., de Wit, C.C., Hagander, P., "Controllability Issues of Robots in Singular Configurations," *Proc. IEEE Int. Conf. on Robotics and Auto.*, pp. 2210–2215, 1991.

[17] Sreenivasan, S.V., Waldron, K.J., Nanua, P., "Closed Form Direct Displacement Analysis of a 6-6 Stewart Platform," *Mech. Mach. Theory*, Vol. 29, No. 6, pp. 855–864, 1994.

[18] K. Tchoń and I. Dulęba, "On inverting singular kinematics and geodesic trajectory generation for robot manipulators," J. of Intelligent and Robotic Systems, Vol. 8, pp. 325–359, 1993.

[19] Uchiyama, M., Iimura, K., Pierrot, F., Dauchez, P., Unno, K., Toyoma, O., "A New Design of a Very Fast 6-DOF Parallel Robot," *Proc. 23rd Int. Symp. on Ind. Robots*, pp. 771–776, 1992.

[20] Wampler, C.W., "Forward Displacement Analysis of General Six-in-Parallel SPS (Stewart) Platform Manipulators Using Soma Coordinates," *Mech. Mach. Theory*, Vol. 31, No. 3, pp. 331–337, 1996.

[21] Zhang, C.D., Song, M.S., "Forward Kinematics of a Class of Parallel (Stewart) Platforms with Closed Form Solutions," *J. Robotic Syst.*, Vol. 9, pp. 93–112, 1992.